

Relaxation Augmented Free Energy Perturbation

Ying-Chih Chiang,¹ Christopher Cave-Ayland,¹ Marley L. Samways,¹ Frank Otto,² and Jonathan W. Essex¹

¹*School of Chemistry, University of Southampton,
Highfield, Southampton, SO17 1BJ, United Kingdom*
²*Department of Chemistry, University College London,
20 Gordon Street, London, WC1H 0AJ United Kingdom*
(Dated: December 15, 2024)

We re-examine the concept of free energy calculation using the single-step free energy perturbation (sFEP) method, often referred to as the Zwanzig equation, which frequently fails to converge due to the problem of insufficient sampling. We find a close resemblance between the operation in sFEP and the Franck-Condon principle in quantum mechanics. The insufficient sampling problem then has a vivid physical interpretation as lacking the subsequent relaxation process after the perturbation. Upon augmenting the traditional sFEP with the relaxation process, the new method gives calculated free energies which agree well with the exact solution for two model systems, shedding new light on the underlying physics in non-equilibrium free energy calculations.

PACS numbers: 05.90.+m, 05.20.-y, 05.20.Gg, 05.70.Ln

Owing to promising applications in drug-design [1], free energy calculations [2, 3] have become one of the major tools for computational biology. Applications range from ligand (drug-like molecules) solubility [4, 5], protein-ligand [6, 7] and protein-protein binding affinities [8], to ligand permeation across membranes or lipid bilayers [9, 10]. These great achievements of applying free energy calculations in biological systems reflect the advances and numerous efforts in constructing accurate force fields [11, 12] as well as in developing enhanced sampling techniques [13, 14], to counteract the insufficient sampling issue [15]. While insufficient sampling is normally associated with the difficulty in capturing a relevant configuration change on performing the perturbation (such as inserting a ligand into a receptor), in this article we will revisit the fundamental theory which is widely employed in many free energy methods, i.e. the single-step free energy perturbation method (sFEP), also known as the Zwanzig equation [3], and reveal that insufficient sampling has a vivid interpretation as lacking a relaxation process following the perturbation.

Consider a model with harmonic oscillators, where the potentials of the initial reference state R and the final perturbed state P are denoted by V_R and V_P respectively as in Fig. 1. The sFEP theory states that the Helmholtz free energy difference (ΔA) between the states P and R is given by an ensemble average performed over state R . That is [3],

$$e^{-\beta\Delta A} = \langle e^{-\beta u} \rangle_R, \quad (1)$$

where $u = V_P - V_R$ and $\langle \dots \rangle_R$ denotes the ensemble average over state R , i.e. the associated sampling draws from the equilibrium distribution of state R . $\beta = 1/k_B T$, with the Boltzmann constant and temperature labeled as k_B and T , respectively. Although Eq. 1 is theoretically correct, its application is typically successful only when the perturbation considered is very small. That is, if

the two states were to sample very similar configuration spaces. The term u , as depicted in Fig. 1, can be viewed as the energy change upon changing the potential from V_R to V_P . In other words, it resembles the excitation (or ionization) energy following a vertical transition in the Franck-Condon principle [16], which assumes that the nuclei are frozen during an electronic transition process. If one views the perturbation as the vertical transition process in the Franck-Condon principle, one sees immediately the problem of sampling: at room temperature the sampled configurations correspond exclusively to the equilibrium of state R and no configurations from the equilibrium of state P are sampled, because V_R and V_P in Fig. 1 are well separated. However, if the system were allowed to evolve after being brought to V_P , the system could relax and sample the equilibrium of the perturbed state P , while the additional energy would be released as heat (denoted as q) to the heat bath, illustrated by the orange curve in Fig. 1. This process reduces the system energy and hence is termed the relaxation process, and the energy released in this process will be termed the relaxation energy.

Following the previous discussion, the relaxation occurs naturally in response to the perturbation. Here we aim to show that the relaxation process is exactly the missing configuration change which needs to be sampled in a free energy calculation, by incorporating relaxation directly into sFEP theory to resolve the problem of insufficient sampling. We begin by proposing to include the relaxation energy q into Eq. 1. This yields,

$$e^{-\beta\Delta A} \sim \langle e^{-\beta(u+q)} \rangle_R, \quad (2)$$

where q denotes the relaxation energy of a single relaxation trajectory, and the average is now performed over trajectories that are initiated from the equilibrium microstates of R . In Eq. 2, $e^{-\beta\Delta A}$ and $e^{-\beta(u+q)}$ are not equal, except for in the low temperature limit ($T \rightarrow 0$).

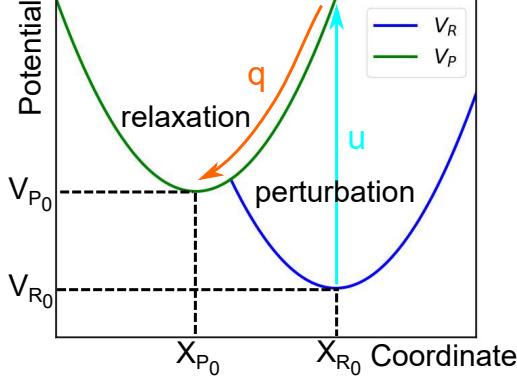


FIG. 1: (color online) Schematic potentials of harmonic oscillator models. The potential of states R and P are labeled as V_R and V_P . The vertical line represents the perturbation u , followed by a relaxation that reduces the energy by releasing heat q . The usual sFEP method contains only the perturbation operation and no relaxation is considered.

In this limit, the population of state R is sharply peaked at the geometry x_{R_0} with the potential minimum V_{R_0} , and all the relaxation trajectories will bring the system to x_{P_0} . The term $u + q$ in Eq. 2 is then equivalent to $V_{P_0} - V_{R_0}$, and hence $\Delta A = V_{P_0} - V_{R_0}$. This result is in line with thermodynamics: there is no entropy contribution to ΔA as $T \rightarrow 0$. Yet, at finite temperature the entropy contribution is no longer zero: relaxation trajectories initiated from a single microstate of R can now end at different microstates of P . That is, there will be many possible relaxation trajectories, starting from the same initial x_R . The effect of this is twofold: First, $e^{-\beta(u+q)}$ fluctuates depending on the sampled relaxation trajectory. Therefore, instead of having a single q , one has to average over all possible q , i.e. average over all possible relaxation trajectories that start from the same initial configuration. As q is dependent on the microstate of P that is sampled, the average over q is effectively an average over P . Second, the fluctuation in q results in a deviation in ΔA evaluated from $e^{-\beta(u+q)}$. Having introduced the ensemble average over P and replaced $u + q$ with $V_P(x') - V_R(x)$ (where x' and x represent the particle position in states P and R , respectively), we have

$$\begin{aligned} e^{-\beta\Delta A'} &= \langle \langle e^{-\beta(u+q)} \rangle_R \rangle_P \\ &= \langle e^{-\beta V_P} \rangle_P \cdot \langle e^{+\beta V_R} \rangle_R, \end{aligned} \quad (3)$$

where $\Delta A'$ is a free-energy-like quantity that deviates from ΔA due to the fluctuation in q . The term $\langle e^{+\beta V_R} \rangle_R$ in Eq. 3 is quite interesting: by definition it reads,

$$\langle e^{+\beta V_R} \rangle_R = \frac{N_R}{Z_R}, \quad (4)$$

where Z_R denotes the partition function of state R and

$$N_R = \int e^{+\beta V_R(x)} e^{-\beta V_R(x)} dx. \quad (5)$$

As the integrand is 1, N_R has a unit of (multi-dimensional) volume. While one may argue that N_R equals the whole volume of space (e.g. size of the box), we note that $e^{-\beta V_R(x)}$ is practically zero where V_R is large. Considering that the ensemble averages are evaluated via sampling, those high-energy regions do not contribute to the ensemble averages. Therefore, to be consistent, we define N_R as the volume of configuration space that is practically accessible during sampling under state R , i.e. the *accessible space volume* of R for abbreviation. Inserting Eq. 4 into Eq. 3, we can rearrange Eq. 3 into

$$\begin{aligned} e^{-\beta\Delta A'} &= \langle e^{-\beta V_P} \rangle_P \cdot \frac{N_R}{Z_R} \cdot \frac{N_P}{N_P} \cdot \frac{Z_P}{Z_P} \\ &= \langle e^{-\beta V_P} \rangle_P \cdot \frac{N_R}{N_P} \cdot \langle e^{+\beta V_P} \rangle_P \cdot e^{-\beta\Delta A}. \end{aligned} \quad (6)$$

To derive the above equation we again utilize the definition of the accessible space volume, i.e. $\langle e^{+\beta V_P} \rangle_P = N_P/Z_P$, and the definition of Helmholtz free energy, i.e. $e^{-\beta\Delta A} = Z_P/Z_R$.

Through Eq. 6, $\Delta A'$ and ΔA are now related. Rearranging Eq. 3 with this key information, we arrive at the final working equation for the relaxation-augmented free energy perturbation (RAFEP), which reads,

$$\begin{aligned} \Delta A &= -\frac{1}{\beta} \ln \frac{\langle \langle e^{-\beta(u+q)} \rangle_R \rangle_P}{\langle e^{-\beta V_P} \rangle_P \cdot \langle e^{+\beta V_P} \rangle_P} + \frac{1}{\beta} \ln \frac{N_R}{N_P} \\ &= \frac{1}{\beta} \ln \langle e^{+\beta V_P} \rangle_P - \frac{1}{\beta} \ln \langle e^{+\beta V_R} \rangle_R + \frac{1}{\beta} \ln \frac{N_R}{N_P} \end{aligned} \quad (7)$$

Interestingly, the final form of Eq. 7 does not depend on the relaxation energy, but solely on properties from the two equilibrium states R and P , demonstrating the feature of A being a state function: the choice of relaxation path has no impact on ΔA ! Therefore, the sampling of microstates can be generated either through a perturbation followed by a relaxation run, or through a direct sampling on the equilibrium of state R and of state P .

As an initial example, we use a system containing two harmonic oscillator potentials with well separated minima, as illustrated in Fig. 1. The parameters used are described in the caption of Fig. 2. Both RAFEP and sFEP calculations were performed using Monte Carlo sampling within a one-dimensional box of 100 Å in length, with 50,000 non-correlated samples collected for both R and P states. The accessible space volume in the RAFEP calculation is obtained from the range of space explored by the particle, taken as the width of the trajectory histogram (the furthest distance between two points observed). Shown in Fig. 2 are results obtained from 50 independent calculations (50 replicas), in comparison to

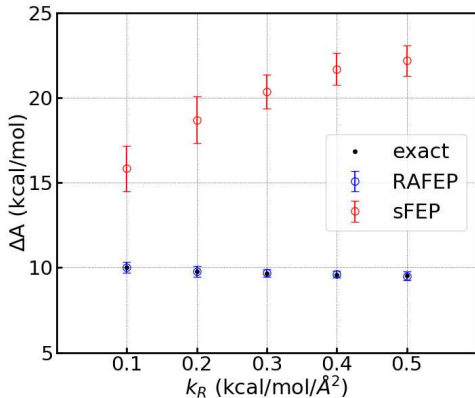


FIG. 2: (Color online) Calculated free energy change for the harmonic oscillator model, using sFEP, RAFEP, and the exact solution. The force constant for state P was taken as 0.1 kcal/mol/Å² in each calculation, while values of 0.1, 0.2, 0.3, 0.4 and 0.5 kcal/mol/Å² were used for state R . A potential trap was engineered by separating the minima by 20 Å in space and 10 kcal/mol in energy. In contrast to sFEP’s poor performance, RAFEP results agree well with the numerical exact solutions, indicating that the potential trap is no longer an issue for RAFEP.

the numerical exact reference calculated by directly evaluating the partition functions of the two states. The standard deviation obtained from 50 replica is depicted as the error bar to indicate the magnitude of statistical fluctuation, i.e. how much the result would deviate when running a single calculation. As expected, the chosen model has a huge potential trap on the reference state which virtually ensures sFEP’s failure in terms of convergence, see e.g. the huge deviation of sFEP (red) from the numerical exact solution (black) in Fig. 2. In contrast, the RAFEP results (blue) always agree well with the numerical exact solution from integrating the partition function, demonstrating that the subsequent relaxation process is indeed the missing configuration change that one should sample during a free energy calculation. Furthermore, the RAFEP results fluctuate less than the sFEP ones, because the convergence no longer depends on serendipity in sampling simultaneously relevant configurations from state P , while performing the sampling under state R . Instead, the relevant configurations from both states are always sampled and used for calculations in RAFEP.

The harmonic oscillator model is a good example for illustrating the concept of introducing relaxation into FEP. Yet, this model contains only a single particle where no interatomic interactions exist. To understand the effect of correlation introduced by the interatomic interaction, we now consider the typical example used in quantum mechanics, that is, particles in a one-dimensional box. The system originally has $N - 1$ Ar atoms inside a 10 Å one-dimensional box, and the goal is to evaluate the free

energy change upon inserting one additional atom. Our examples range from low to high particle densities, where sFEP eventually becomes invalid, and the Lennard-Jones parameters ($\epsilon = 0.238$ kcal/mol and $\sigma = 3.405$ Å) are taken from literature [17]. Starting from $N = 2$, the two Ar atoms are initially non-interacting in state R , echoed in the non-correlated 2-dimensional histogram obtained from Monte Carlo (MC) sampling where the entire box is accessible by both atoms, see Fig. 3(a). In contrast, these two Ar atoms in state P repel each other at short interatomic distances due to their Lennard-Jones interaction, and the MC trajectory yields a correlated histogram as shown in Fig. 3(b). Clearly, the accessible space volume differs between states R and P : the former is L^2 and the latter $(L - d)^2$, where L and d stand for the box size and the intercept of the white area with the axis in Fig. 3(b), respectively. In the limit of the low density condition (such as this two atom case), it transpires that this change in volume is the dominant contribution to ΔA . The accessible space volume in general can be evaluated either via a histogram method or via direct integration. The former calculates the volume based on the occupancy of a multi-dimensional trajectory histogram as shown in Fig. 3(a-b), and the latter directly calculates the volume by the sum of all histogram bins whose Boltzmann weight of the centroid configuration is larger than 0.1% of the largest weight. The 0.1% cutoff was an estimation obtained from the histogram method for the $N = 2$ example.

Results of the free energy change, calculated using sFEP and RAFEP, for the insertion of a single atom into a box containing varying numbers of atoms are shown in Fig. 3(c). The numerical exact reference was obtained via the multi-step free energy perturbation method [18] in combination with Barnett acceptance ratio [19] (mFEP-BAR), which was performed using 100 windows (each with 2,000,000 MC steps) and soft-core potentials [20] ($\alpha = 0.1$ for Lennard-Jones particles) to obtain converged mFEP-BAR reference data for $N = 5$. The allowed MC moves include the usual translational moves with a step size up to 0.25 Å and position swaps of two atoms at a move ratio of 3:7. This protocol was confirmed by comparing the results to that obtained from evaluation of the partition functions up to $N = 4$. This elaborated protocol illustrates the difficulty in getting the correct ΔA under an extreme case for $N = 5$. In contrast, the MC sampling in sFEP calculations requires only one window, without the soft-core potential. The RAFEP calculations were performed by collecting microstates as in the sFEP sampling of state R , and from each microstate a 10,000 MC step simulation is performed to yield the equilibrium microstate for state P . It would also be possible to simply collect the equilibrium microstates of P , rather than explicitly simulating the relaxation process. Our operation is only to demonstrate how the relaxation moves can be performed via the traditional MC sampling. As shown in

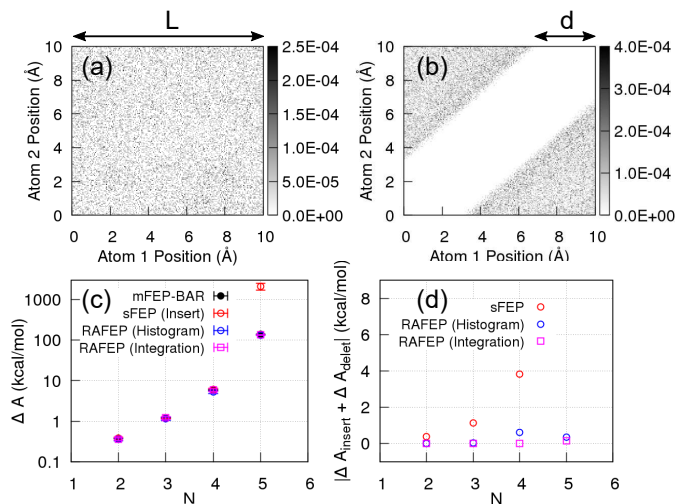


FIG. 3: (Color online) (a) The trajectory histogram obtained during sampling the state R for $N = 2$. The histogram is obtained using a bin width of 0.05 \AA and normalized with respect to the number of trajectory frames. The two atoms are uncorrelated and both can populate the whole box space. This gives an accessible space volume as expected, i.e. L^2 . (b) The trajectory histogram of state P for $N = 2$. The two atoms are correlated and thus repel each other at short interatomic distances. The outcome is the unpopulated area in white and an accessible space volume of $(L - d)^2$ throughout the sampling. This volume is notably smaller than in panel (a), and therefore the entropy reduces (ΔA increases) upon performing the perturbation. (c) Free energy changes associated with inserting one atom into systems containing varying numbers of atoms ($N - 1$ atoms), calculated using sFEP, RAFEP, and mFEP-BAR. As can be seen the sFEP results diverge dramatically from the mFEP-BAR reference at $N = 5$, which is not observed in RAFEP calculations. (d) Free energy change in a closed cycle. One atom is removed and then inserted back in the system. Summing up the free energy change of the former (ΔA_{delete}) operation and the latter (ΔA_{insert}) should be zero. The sFEP results are known to deviate from zero heuristically, especially for $N = 5$ where the result is 2000 kcal/mol off. In comparison, RAFEP generally shows the same performance in particle deletion and insertion operations.

Fig. 3(c), sFEP (red) performs badly when $N = 5$ (with an error of ~ 2000 kcal/mol), whereas RAFEP (blue and magenta) always follow closely the exact numerical reference. The deviation of RAFEP from the reference results (up to 1 kcal/mol and 7 kcal/mol for $N = 4$ and $N = 5$, respectively) is observed when calculating the accessible space volume via the trajectory histogram method, owing to the insufficient population of the histogram bins. For instance, if 20 bins are employed for each degree of freedom, one needs to distribute 20,000 trajectory points among 160,000 bins for $N = 4$ case. This problem can be resolved by using the numerical integration to calculate the volume (see e.g. the magenta data in Fig. 3(c)), yielding significantly more accurate results.

The last thing we would like to discuss is the hysteresis phenomenon that is often observed in sFEP calculations for operations along a closed path. To do so, one atom from the system is first removed and then inserted again. The free energy change of the former (deletion) and the latter (insertion) should bear the same magnitude but with opposite sign. Thus, the free energy change of the entire cycle should be zero. Heuristically it is known that sFEP performs better for insertion than for deletion [21], so the net change of ΔA is normally not zero, as depicted by the red circles in Fig. 3(d). In contrast, RAFEP results (especially those obtained with volume integration) are very close to zero. This is understandable: the relaxation effect is more relevant in a deletion calculation, because this perturbation creates a void. For atoms next to this void, their interatomic distance is then larger than in equilibrium conditions. On the contrary, an insertion would not create a void, so no relaxation process is required, unless the system has a very high particle density where the environment needs to reorganize to accommodate the new atom. Since RAFEP always explicitly includes the relaxation in its sampling, it is not surprising that it performs equally well in both cases.

In this letter, we have re-examined the origin of the insufficient sampling encountered in a sFEP calculation and discovered that the relaxation processes are the key to the missing relevant configurations and can be included in free energy calculations via Eq. 7. While there are methods echoing our nonequilibrium approach, e.g. nonequilibrium candidate Monte Carlo method (NCMC) [22], the nonequilibrium molecular dynamics Monte Carlo (neMD/MC) [23], and Jarzynski's equality [24], some of their underlying theory employs the detailed balance condition – an equilibrium condition that nullifies the effort in employing the relaxation information. As a consequence, heuristically it was found that their best performance occurs when calculations are performed over many steps/windows, within each a quasi-equilibrium condition holds. Owing to the curse of dimensionality, RAFEP with the multi-dimensional histogram method currently cannot be applied to complex systems. Yet we hope that the physics revealed here would stimulate new methods to be developed to fully harness the power of the nonequilibrium relaxation process, following a single large perturbation.

Acknowledgment

YCC thanks the Royal Society for funding this research (Newton International Fellowship, NF171278) and iSolution at the University of Southampton for computing time on the Iridis4 cluster.

-
- [1] Z. Cournia, B. Allen, and W. Sherman, *Journal of Chemical Information and Modeling* **57**, 2911 (2017).
- [2] J. G. Kirkwood, *The Journal of Chemical Physics* **3**, 300 (1935).
- [3] R. W. Zwanzig, *The Journal of Chemical Physics* **22**, 1420 (1954).
- [4] D. L. Mobley, C. I. Bayly, M. D. Cooper, M. R. Shirts, and K. A. Dill, *Journal of Chemical Theory and Computation* **5**, 350 (2009).
- [5] J. L. Knight, J. D. Yesselman, and C. L. Brooks, *Journal of Computational Chemistry* **34**, 893 (2013).
- [6] L. Wang, B. J. Berne, and R. A. Friesner, *Proceedings of the National Academy of Sciences* **109**, 1937 (2012).
- [7] L. Wang et al., *Journal of the American Chemical Society* **137**, 2695 (2015).
- [8] J. C. Gumbart, B. Roux, and C. Chipot, *Journal of Chemical Theory and Computation* **9**, 3789 (2013).
- [9] D. Bemporad, C. Luttmann, and J. W. Essex, *Biophysical Journal* **87**, 1 (2004).
- [10] J. Comer, K. Schulten, and C. Chipot, *Journal of Chemical Theory and Computation* **13**, 2523 (2017).
- [11] J. A. Maier et al., *Journal of Chemical Theory and Computation* **11**, 3696 (2015).
- [12] J. Huang et al., *Nature Methods* **14**, 71 (2017).
- [13] A. Laio and M. Parrinello, *Proceedings of the National Academy of Sciences* **99**, 12562 (2002).
- [14] Y. Sugita and Y. Okamoto, *Chemical Physics Letters* **314**, 141 (1999).
- [15] D. L. Mobley, J. D. Chodera, and K. A. Dill, *Journal of Chemical Theory and Computation* **3**, 1231 (2007).
- [16] G. Herzberg, *Molecular Spectra and Molecular Structure - Vol 1*, D. Van Nostrand Company, Inc., Princeton, New Jersey, USA, 2nd edition, 1950.
- [17] D. Frenkel and B. Smit, *Understanding Molecular Simulation*, Academic Press, Inc., Orlando, FL, USA, 2nd edition, 2001.
- [18] J. P. Valleau and D. N. Card, *The Journal of Chemical Physics* **57**, 5457 (1972).
- [19] C. H. Bennett, *Journal of Computational Physics* **22**, 245 (1976).
- [20] M. Zacharias, T. P. Straatsma, and J. A. McCammon, *The Journal of Chemical Physics* **100**, 9025 (1994).
- [21] N. Lu and D. A. Kofke, *The Journal of Chemical Physics* **114**, 7303 (2001).
- [22] J. P. Nilmeier, G. E. Crooks, D. D. L. Minh, and J. D. Chodera, *Proceedings of the National Academy of Sciences* **108**, E1009 (2011).
- [23] B. K. Radak and B. Roux, *The Journal of Chemical Physics* **145**, 134109 (2016).
- [24] C. Jarzynski, *Phys. Rev. Lett.* **78**, 2690 (1997).